Acta Polytechnica **64**(2):128–141, 2024
https://doi.org/10.14311/AP.2024.64.0128

Published by the Czech Technical University in Prague

NUMERICAL SOLUTION FOR STOCHASTIC VOLTERRA-FREDHOLM INTEGRAL EQUATIONS WITH DELAY ARGUMENTS

Kutorzi Edwin Yao[a,b], Yuxue Zhang[a,b], Yufeng Shi[a,b,*]

[a] *Shandong University, Institute for Financial Studies, 250100 Jinan, China*

[b] *Shandong University, School of Mathematics, 250100 Jinan, China*

[*] corresponding author: yfshi@sdu.edu.cn

Abstract. We present a method for computing the stochastic operational matrix of integration to advance the study of stochastic Volterra-Fredholm integral equations (SVFIEs) based on delay arguments. First, the method evaluates the combined effects of the delay and its parameters on the accuracy improvement of the convergence rate. Our results can be applied to SVFIEs, with the operational delay matrices of the block pulse function simplified to algebraic ones. Numerical calculations were performed on a PC using Python 3 programs. Results also demonstrate the accuracy of approximate solutions; arithmetic operations are carried out without the need for derivation or integration.

Keywords: Stochastic Volterra-Fredholm integral equations, block-pulse functions, Itô integral, delay operational matrix, error analysis.

1. Introduction

Stochastic Volterra-Fredholm integral equations are an essential class of multi-dimensional integral equations that can rarely be solved exactly, and the computational complexity of mathematical operations is a critical obstacle in solving high-dimensional stochastic integral equations. Stochastic differential equations have various applications in various fields, such as medicine, economics, and social sciences, as well as engineering, biology, and financial mathematics. These equations play a crucial role in modelling population growth, where the stochastic Volterra-Fredholm integral equation is fundamental; see [1–7]. A stochastic Volterra-Fredholm integral equations can be modeled using several types of stochastic differential equations or, in more complicated cases, nonlinear stochastic differential equations of the Itô type [8–10]. There are some difficulties in finding exact solutions for SVIEs or SVFIEs, so the researchers have resorted to finding approximate solutions using numerical methods [11, 12].

SVFIEs with delay are used in applied sciences for modelling functions that contain time memory, such as mechanical systems, dynamical systems, and electric circuits, as well as in physical models, option pricing, and population growth [13]. On the one hand, in the theory of automatic systems, delay-differential equations are obtained [14–16].

On the other hand, some systems, such as the integral equations [17, 18], which were based on the operational matrices of integration, were estimated using polynomials. These included block pulse systems, the Fourier series, Legendre polynomials, Chebyshev polynomials, and Laguerre polynomials. Using numerical methods to approximate the solutions to such equations is often desirable since they cannot always be solved explicitly [19–27]. The Volterra integral equations with delay have received very little attention. We have developed approximation methods for SVFIEs with delay arguments. A stochastic operational matrix with time delay is presented to find an approximate solution of the Stochastic Volterra-Fredholm integral equations.

Our focus is on the SVFIE:

$$X(t) = f(t) + \lambda_1 \int_\alpha^\beta k_1(t,s)X(s-\tau)ds + \lambda_2 \int_0^t k_2(t,s)X(s-\tau)ds + \lambda_3 \int_0^t k_3(t,s)X(s-\tau)dB(s),$$

where $t \in [0,T)$, $\tau \in [\alpha,\beta]$, $\tau \in [0,t)$.

In the above descriptions, $X(t)$, $f(t)$, $k_1(t,s)$, $k_2(t,s)$ and $k_3(t,s)$, for $t,s \in [0,T)$, are the stochastic processes defined on the same probability space $(\Omega,\mathcal{F},\mathbb{P})$, and $X(t)$ is unknown. $B(t)$ is a one-dimensional standard Brownian motion process and $\int_0^t k_3(t,s)X(s-\tau)dB(s)$ is the Itô integral. Both the j and k represent the Volterra kernel. The parameter in the variable of the function is calculated as $\tau = (q+\lambda)h$ with an integer $q \geq 0$ and a fraction $0 \leq \lambda < 1$, chosen to approximate a function with a time delay.

Following is an outline of the paper. A description of the fundamental properties of block-pulse functions is provided in Section 2, as well as the approximation of functions using block-pulse parts and an operational

integration matrix. A stochastic integration functional matrix is introduced in Section 3. The stochastic integration active matrix is used to solve stochastic delay Volterra integral equations in Section 4. We present the error estimation and rate of convergence in Section 5. The proposed scheme is accurate, which is proved by using numerical examples to demonstrate its effectiveness in Section 6. A brief conclusion is given in Section 7.

2. Block-pulse functions (BPFs)

This section covers the notations, definitions, known results, and formulas related to BPFs, which are relevant to this paper. These details have been extensively discussed in [20, 21].

The block-pulse functions (BPF) Φ_i over the unit interval $[0,1)$ is defined as follows: for $0 \leq i < m$, and $m \in \{1,2,\ldots\}$:

$$\Phi_i(t) = \begin{cases} 1 & (i-1)h \leq t < ih, \\ 0 & \text{otherwise}, \end{cases} \tag{1}$$

with $t \in [0,T)$, $i = 1,2,\ldots,m$, and $h = \frac{T}{m}$.

The block-pulse functions have the following properties:

(1.) Disjointness: The BPFs are disjointed with each other in the interval $t \in [0,T)$:

$$\Phi_i(t)\Phi_j(t) = \delta_{ij}\Phi_i(t), \tag{2}$$

where $i,j = 1,2,\ldots,m$, and δ_{ij} denotes the Kronecker delta.

(2.) Orthogonality: The BPFs are orthogonal with each other in the interval $t \in [0,T)$:

$$\int_0^T \Phi_i(t)\Phi_j(t)dt = h\delta_{ij}, \tag{3}$$

where $i,j = 1,2,\ldots,m$.

(3.) The third property is completeness: For every $f \in L^2[0,T)$, when $m \to \infty$, Parseval's identity holds, that is:

$$\int_0^T f^2(t)dt = \sum_{i=1}^{\infty} f_i^2 ||\Phi_i(t)||^2,$$

where $f_i = \frac{1}{h}\int_0^T f(t)\Phi_i(t)dt$.

The set of functions can be described by an m vector:

$$\Phi(t) = (\Phi_0(t), \Phi_1(t), \cdots, \Phi_m(t))^T,$$

where $t \in [0,T)$.

Thus, we can write the relationship between BPFs and their integrals in the following matrix form. The above representation and disjointness property follows:

$$\Phi(t)\Phi^T(t) = \begin{pmatrix} \Phi_1(t) & 0 & \cdots & 0 \\ 0 & \Phi_2(t) & \cdots & 0 \\ \vdots & \vdots & \ddots & \vdots \\ 0 & 0 & \cdots & \Phi_m(t) \end{pmatrix}_{m\times m}, \tag{4}$$

additionally, we deduce:

$$\Phi^T(t)\Phi(t) = 1,$$

and:

$$\Phi(t)\Phi^T(t)F^T = D_F\Phi(t), \tag{5}$$

the diagonal matrix D_F corresponds to a constant vector $F = (f_1, f_2, \cdots, f_m)^T$ whose diagonal entries are related.

2.1. Functions approximation

A real bounded function $f(t)$, which $f(t) \in L^2[0,T)$, can be expanded into a block pulse series as:

$$f(t) \simeq \hat{f}_m(t) = \sum_{i=1}^{m} f_i \Phi_i(t), \tag{6}$$

where f_i is the block pulse coefficient with respect to the ith BPF $\Phi_i(t)$. The vector form is as follows:

$$f(t) \simeq \hat{f}_m(t) = F^T \Phi(t) = \Phi^T(t) F, \tag{7}$$

where $F = (f_1, f_2, \cdots, f_m)^T$.

Let $k(t,s) \in L^2([0,T_1) \times [0,T_2))$. Similarly, it can be applied to BPFs such as:

$$k(t,s) \simeq \hat{k}_m(t,s) = \Psi^T(s) K \Phi(t) = \Phi^T(t) K^T \Psi(s), \tag{8}$$

where $\Phi(t)$ and $\Psi(s)$ are m_1 and m_2 dimensional BPFs vectors, respectively, and $K = (k_{ij})$, $i = 1, 2, \ldots, m_1$, $j = 1, 2, \ldots, m_2$ is the $m_1 \times m_2$ block pulse coefficient matrix with:

$$k_{ij} = \frac{1}{h_1 h_2} \int_0^{T_1} \int_0^{T_2} k(t,s) \Psi_i(t) \Phi_j(s) ds dt,$$

where $h_1 = \frac{T_1}{m_1}, h_2 = \frac{T_2}{m_2}$. For convenience, we put $m_1 = m_2 = m$.

2.2. Integration operational matrix

Computing $\int_0^t \Phi_i(s) ds$ follows:

$$\int_0^t \Phi_i(s) ds = \begin{cases} 0 & 0 \le t < (i-1)h, \\ t - (i-1)h & (i-1)h \le t < ih, \\ h & ih \le t < T. \end{cases} \tag{9}$$

Note that $t - (i-1)h$, equals to $\frac{h}{2}$ at mid-point of $[(i-1)h, ih)$, thus we can approximate $t - (i-1)h$, for $(i-1)h \le t < ih$, by $\frac{h}{2}$.

From [20], we have:

$$\int_0^t \Phi(s) ds = P \Phi(t). \tag{10}$$

As shown in the operational matrix of integration:

$$P = \frac{h}{2} \begin{pmatrix} 1 & 2 & 2 & \cdots & 2 \\ 0 & 1 & 2 & \cdots & 2 \\ 0 & 0 & 1 & \cdots & 2 \\ \vdots & \vdots & \vdots & \ddots & \vdots \\ 0 & 0 & 0 & \cdots & 1 \end{pmatrix}_{m \times m} \tag{11}$$

Accordingly, each integral of $f(t)$ can be approximated as follows:

$$\int_0^t f(s) ds \simeq \int_0^t F^T \Phi(s) ds \simeq F^T P \Phi(t). \tag{12}$$

2.3. The operational matrix with time delay of BPFs

The delay time is $\tau = (q + \lambda)h$ with an integer $q \ge 0$, and a fraction $0 \le \lambda < 1$, where the operational matrix of approximation is expressed as the time delay $\tau = qh$, yields:

$$\phi_i(t - qh) = \begin{cases} \phi_{i+q}(t) & i \le m - q, \\ 0 & i > m - q, \end{cases} \tag{13}$$

and the function containing time delay, yields:

$$\phi_i(t - \tau) = \begin{cases} \phi_{i+q}(t) + \phi_\lambda(t - (i+q)h) - \phi_\lambda(t - (i+q-1)h) & i < m - q, \\ \phi_{i+q}(t) - \phi_\lambda(t - (i+q-1)h) & i = m - q, \\ 0 & i > m - q, \end{cases} \tag{14}$$

alternatively, as vectors:

$$\phi_i(t-\tau) = \Delta_i^T H^q \Phi(t) - \Delta_i^T H^q \Phi_\lambda(t) + \Delta_i^T H^{q+1} \Phi_\lambda(t).$$

We expand the function $\phi_i(t-\tau)$ into its block pulse series to avoid the expression $\Phi_\lambda(t)$ in the above equation:

$$\phi_i(t-\tau) = (c_{i,1} \quad c_{i,2} \cdots c_{i,m})\Phi(t) \tag{15}$$

While $c_{i,j}$ $(j = 1, 2 \cdots, m)$ are:

$$\begin{aligned} c_{i,j} &= \frac{1}{h}\int_0^T \phi_i(t-\tau)\phi_j(t)dt = \frac{1}{h}\int_{(j-1)h}^{jh} \phi_i(t-\tau)dt \\ &= \frac{1}{h}\Delta_i^T H^q \left(\int_{(j-1)h}^{jh} \Phi(t)dt - \int_{(j-1)h}^{jh} \Phi_\lambda(t)dt + H\int_{(j-1)h}^{jh} \Phi_\lambda(t)dt \right) \\ &= \Delta_i^T((1-\lambda)H^q + \lambda H^{q+1})\Delta_j. \end{aligned} \tag{16}$$

We can develop the whole block pulse function vector containing time delay $\tau = (q+\lambda)h$ into its block pulse series in a vector form by noting that the expression $\Delta_i^T((1-\lambda)H^q + \lambda H^{q+1})\Delta_j$ is just one entry of the matrix $((1-\lambda)H^q + \lambda H^{q+1})$ with ith row and jth column:

$$\Phi(t-\tau) = ((1-\lambda)H^q + \lambda H^{q+1})\Phi(t). \tag{17}$$

Usually, the matrix $(1-\lambda)H^q + \lambda H^{q+1}$ is referred to as the delay operational matrix. To put it in more concrete terms:

$$(1-\lambda)H^q + \lambda H^{q+1} = \begin{pmatrix} & & & \overbrace{\quad}^{(q+1)th} & & & & \\ 0 & \cdots & 0 & 1-\lambda & \lambda & 0 & \cdots & 0 \\ 0 & \cdots & 0 & 0 & 1-\lambda & \lambda & \cdots & 0 \\ \vdots & \cdots & \vdots & \vdots & \vdots & \vdots & \ddots & \vdots \\ 0 & \cdots & 0 & 0 & 0 & 0 & \cdots & \lambda \\ 0 & \cdots & 0 & 0 & 0 & 0 & \cdots & 1-\lambda \\ 0 & \cdots & 0 & 0 & 0 & 0 & \cdots & 0 \\ \vdots & \cdots & \vdots & \vdots & \vdots & \vdots & \cdots & \vdots \\ 0 & \cdots & 0 & 0 & 0 & 0 & \cdots & 0 \end{pmatrix}. \tag{18}$$

It is possible to obtain the block pulse series of a function with time delay $\tau = (q+\lambda)h$ by using Equation (17):

$$f(t-\tau) \simeq F^T\Phi(t-\tau) = F^T((1-\lambda)H^q + \lambda H^{q+1})\Phi(t). \tag{19}$$

3. Stochastic integration operational matrix

The integral of Itô of a single BPF $\phi_i(t)$ can be computed as follows:

$$\int_0^t \phi_i(s)dB(s) = \begin{cases} 0 & 0 \le t < (i-1)h, \\ B(t) - B((i-1)h), & (i-1)h \le t < ih, \\ B(ih) - B((i-1)h), & ih \le t < T. \end{cases} \tag{20}$$

Now expressing $\int_0^t \phi_i(s)dB(s)$, in terms of the BPFs follows:

$$\int_0^t \phi_i(s)dB(s) \simeq (B(ih/2) - B(i-1)h/2)\,\phi_i(t) + (B(ih) - B((i-1)h)) \sum_{j=i+1}^{m} \phi_j(t). \tag{21}$$

Therefore:

$$\int_0^t \Phi(s)dB(s) \simeq P_S\Phi(t). \tag{22}$$

In this case, the stochastic operational matrix of integration can be expressed as follows:

$$P_S = \begin{pmatrix} \gamma_1 & \rho_1 & \rho_1 & \cdots & \rho_1 \\ 0 & \gamma_2 & \rho_2 & \cdots & \rho_2 \\ 0 & 0 & \gamma_3 & \cdots & \rho_3 \\ \vdots & \vdots & \vdots & \ddots & \vdots \\ 0 & 0 & 0 & \cdots & \gamma_m \end{pmatrix}_{m\times m}, \tag{23}$$

where $\rho_i = B(ih) - B((i-1)h)$, $i = 1, 2, \ldots, m-1$; $\gamma_j = B(ih/2) - B((i-1)h/2)$, $j = 1, 2, \ldots, m$.

This can be approximated by computing the Itô integral for every function $f(t)$ as follows:

$$\int_0^t f(s)dB(s) \simeq F^T\Phi(s)dB(s) \simeq F^T P_S \Phi(t). \tag{24}$$

4. Solving stochastic Volterra-Fredholm integral equations with time delay

The following linear stochastic Volterra-Fredholm integral equation is considered with a constant time delay $\tau > 0$:

$$X(t) = f(t) + \lambda_1 \int_\alpha^\beta k_1(t,s)X(s-\tau)ds + \lambda_2 \int_0^t k_2(t,s)X(s-\tau)ds + \lambda_3 \int_0^t k_3(t,s)X(s-\tau)dB(s), \tag{25}$$

where $t \in [\alpha, \beta]$, $\tau \in (0, \beta - \alpha)$, $t \in [0, T)$.

$X(t)$ is a stochastic process whose coefficients are $X(t)$, $f(t)$, $k_1(t,s)$, $k_2(t,s)$ and $k_3(t,s)$, for $\alpha, \beta \in [\alpha, \beta]$, $t, s \in [0, T)$, defined on the same probability space $(\Omega, \mathcal{F}, P)$. In addition, $B(t)$ is a Brownian motion process, and $\int_0^t k_3(t,s)X(s-\tau)dB(s)$ is integral for Itô. To facilitate block pulse functions, we typically set $\alpha = 0$. Whenever $\alpha \neq 0$ we set $s = \frac{t-\alpha}{\beta-\alpha}T$, where $T = mh$. Using BPFs to approximate functions $X(t)$, $f(t)$, $K_1(t,s)$, $K_2(t,s)$, and $K_3(t,s)$ by Equations (7), (8), and (19) gives the following result:

$$\begin{cases} X(t) \simeq X^T\Phi(t) = \Phi^T X, \\ f(t) \simeq F^T\Phi(t) = \Phi^T F, \\ k_1(t,s) \simeq \Psi^T(t)K_1\Phi(s) = \Phi^T(s)K_1^T\Psi(t), \\ k_2(t,s) \simeq \Psi^T(t)K_2\Phi(s) = \Phi^T(s)K_2^T\Psi(t), \\ k_3(t,s) \simeq \Psi^T(t)K_3\Phi(s) = \Phi^T(s)K_3^T\Psi(t). \end{cases}$$

According to Equation (19), $X(s-\tau)$ can be approximated as follows:

$$X(s-\tau) \simeq X^T\Psi(s-\tau) = X^T((1-\lambda)H^q + \lambda H^{q+1})\Phi(t)\Psi(s),$$

and by letting $Z = ((1-\lambda)H^q + \lambda H^{q+1})$, we can write:

$$X(s-\tau) \simeq X^T Z\Psi(s). \tag{26}$$

The above approximates define X and F as stochastic block pulse coefficients vectors, respectively, and K_1, K_2, and K_3 as stochastic block pulse coefficients matrices.

Equation (25) is improved by substituting the above approximation:

$$\begin{aligned} X^T\Phi(t) \simeq F^T\Phi(t) &+ X^T Z(\lambda_1 \int_0^{mh} \Psi(s)\Psi^T(s)ds)K_1\Phi(t) \\ &+ X^T Z(\lambda_2 \int_0^t \Psi(s)\Psi^T(s)ds)K_2\Phi(t) \\ &+ X^T Z(\lambda_3 \int_0^t \Psi(s)\Psi^T(s)dBs)K_3\Phi(t). \end{aligned} \tag{27}$$

Let K_j^i, $j = 1, 2, 3$, be the ith row of the constant matrix K_j, for $j = 1, 2, 3$. R^i be the ith row of the integration operational matrix P, R_S^i be the ith row of the stochastic integration operational matrix $P_S, D_{K_j^i}$, be diagonal matrices with K_j^i, for $j = 1, 2, 3$, as its diagonal entries. By the relation $\int_0^{mh} \Phi^T\Phi(s)ds = hI$, previous relations, and assuming $m_1 = m_2$, we have:

$$\left(\int_0^{mh} \Psi(s)\Psi^T(s)ds\right) K_1\Phi(t) = hIK_1\Phi(t) = B_1\Phi(t), \tag{28}$$

where $B_1 = hK_1$, also:

$$\begin{aligned}\left(\int_0^t \Psi(s)\Psi^T(s)ds\right) K_1\Phi(t) &= \left(\int_0^t \Phi(s)\Phi^T(s)ds\right) K_2\Phi(t)\\ &= \begin{pmatrix} R^1\Phi(t)K_2^1\Phi(t)\\ R^2\Phi(t)K_2^2\Phi(t)\\ \vdots\\ R^m\Phi(t)K_2^m\Phi(t)\end{pmatrix} = \begin{pmatrix} R^1D_{K_2^1}\\ R^2D_{K_2^2}\\ \vdots\\ R^mD_{K_2^m}\end{pmatrix}\Phi(t)\\ &= B_2\Phi(t),\end{aligned} \tag{29}$$

where:

$$B_2 = \frac{h}{2}\begin{pmatrix} k_{11}^2 & 2k_{12}^2 & 2k_{13}^2 & \cdots & 2k_{1m}^2\\ 0 & k_{22}^2 & 2k_{23}^2 & \cdots & 2k_{2m}^2\\ 0 & 0 & k_{33}^2 & \cdots & 2k_{3m}^2\\ \vdots & \vdots & \vdots & \ddots & \vdots\\ 0 & 0 & 0 & \cdots & k_{mm}^2\end{pmatrix}_{m\times m}, \tag{30}$$

also, we can consider the integral term Itô:

$$\begin{aligned}\left(\int_0^t \Psi(s)\Psi^T(s)dB(s)\right) K_3\Phi(t) &= \left(\int_0^t \Phi(s)\Phi^T(s)dB(s)\right) K_3\Phi(t)\\ &= \begin{pmatrix} R^1\Phi(t)K_3^1\Phi(t)\\ R^2\Phi(t)K_3^2\Phi(t)\\ \vdots\\ R_S^m\Phi(t)K_3^m\Phi(t)\end{pmatrix} = \begin{pmatrix} R_S^1D_{K_3^1}\\ R_S^2D_{K_3^2}\\ \vdots\\ R_S^mD_{K_3^m}\end{pmatrix}\Phi(t)\\ &= B_3\Phi(t),\end{aligned} \tag{31}$$

where:

$$B_3 = \begin{pmatrix} k_{11}^3\gamma & k_{12}^3\rho & k_{13}^3\rho & \cdots & k_{1m}^3\rho\\ 0 & k_{22}^3\gamma & k_{23}^3\rho & \cdots & k_{2m}^3\rho\\ 0 & 0 & k_{33}^3\gamma & \cdots & k_{3m}^3\rho(m-2)\\ \vdots & \vdots & \vdots & \ddots & \vdots\\ 0 & 0 & 0 & \cdots & k_{mm}^3\gamma(m-1)\end{pmatrix}. \tag{32}$$

By substituting Equations (28), (29) and (31) in (27), we get:

$$X^T\Phi(t) \simeq F^T\Phi(t) + X^TZ\lambda_1B_1\Phi(t) + Y^TZ\lambda_2B_2\Phi(t) + X^TZ\lambda_3B_3\Phi(t).$$

Then:

$$X^T(I - Z(\lambda_1B_1 + \lambda_2B_2 + \lambda_3B_3)) \simeq F^T.$$

So, by setting $M = (I - Z(\lambda_1B_1 + \lambda_2B_2 + \lambda_3B_3))$ and replacing $\simeq$ by $=$, we deduce:

$$M^TX = F. \tag{33}$$

It consists of a linear system of equations with lower triangular coefficients that yields the approximate block pulse coefficient of the stochastic process $X(t)$.

5. Error estimation and rate of convergence

The proposed method shows the fastest convergence rate for integral equations with time delay. There is a high-level agreement between the exact solution and numerical results.

Theorem 1. Let $f(t)$ be any arbitrary real bounded function, which is square integrable within the interval $[0,1)$, and $e(t) = f(t) - \hat{f}_m(t), t \in I = [0,1)$, where $\hat{f}_m(t) = \sum_{i=1}^m f_i\phi_i(t)$ is the block pulse series of $f(t)$. Then:

$$\|e(t)\| \leq \frac{h}{2\sqrt{3}}\|f'\|_\infty, \tag{34}$$

in this case, $\|e(t)\| = \left(\int_0^1 |e(t)|^2\,dt\right)^{\frac{1}{2}}$.

Proof. See [23].

Theorem 2. Assume $f(t,s) \in L^2([0,1)\times[0,1))$ and $e(t,s) = f(t,s) - \hat{f}_m(t,s)$, $(t,s) \in A = [0,1)\times[0,1)$, which $\hat{f}_m(t,s) = \sum_{i=1}^{m}\sum_{j=1}^{m} f_{ij}\Psi_i(t)\Phi_j(s)$ is the block pulse series of $f(t,s)$. Then:

$$\|e(t,s)\| \leq \frac{h}{2\sqrt{3}}\left(\|f_t'\|_\infty^2 + \|f_t'\|_\infty^2\right)^{\frac{1}{2}}, \tag{35}$$

where $\|e(t,s)\| = \left(\int_0^1\int_0^1 |e(t,s)|^2 dsdt\right)^{\frac{1}{2}}$.

Proof. Let:

$$e_{ij}(t,s) = \begin{cases} f(t,s) - f_{ij} & (t,s)\in A_{ij}, \\ 0 & (t,s)\in A - A_{ij}, \end{cases} \tag{36}$$

where $A_{ij} = \{(t,s) : (i-1)h \leq t < ih, (j-1)h \leq s < jh, h = \frac{1}{m}\}$, and $i,j = 1,2,\cdots,m$. For $i,j = 1,2,\cdots,m$, thus, we get:

$$e_{ij}(t,s) = f(t,s) - \frac{1}{h^2}\int_{(i-1)h}^{ih}\int_{(j-1)h}^{jh} f(x,y)dydx = \frac{1}{h^2}\int_{(i-1)h}^{ih}\int_{(j-1)h}^{jh}\left(f(t,s) - f(x,y)\right)dydx,$$

now, by mean-value theorem, we deduce:

$$\begin{aligned} e_{ij}(t,s) &= \frac{1}{h^2}\int_{(i-1)h}^{ih}\int_{(j-1)h}^{jh}\left((t-x)f_t'(\eta_i,\eta_j) + (s-y)f_s'(\eta_i,\eta_j)\right)dydx \\ &= f_t'(\eta_i,\eta_j)\left(t + \left(-i+\frac{1}{2}\right)h\right) + f_s'(\eta_i,\eta_j)\left(s + \left(-j+\frac{1}{2}\right)h\right), \end{aligned}$$

where $(t,s),(\eta_i,\eta_j) \in A_{ij}$; then:

$$\|e_{ij}(t,s)\|^2 = \int_{(i-1)h}^{ih}\int_{(j-1)h}^{jh} |e_{ij}(t,s)|^2\, dsdt = \frac{h^4}{12}(f_t'^2(\eta_i,\eta_j) + f_s'^2(\eta_i,\eta_j)), \tag{37}$$

where $(\eta_i,\eta_j) \in A_{ij}$, $i,j = 1,2,\ldots,m$.

Consequently, we have:

$$\begin{aligned} \|e(t,s)\|^2 &= \int_0^1\int_0^1 |e(t,s)|^2\, dsdt = \int_0^1\int_0^1\left(\sum_{i=1}^{m}\sum_{j=1}^{m} e_{ij}(t,s)\right)^2 dsdt \\ &= \sum_{i=1}^{m}\sum_{j=1}^{m}\int_0^1\int_0^1 e_{ij}^2(t,s)dsdt = \sum_{i=1}^{m}\sum_{j=1}^{m}\|e_{ij}(t,s)\|^2 \\ &= \frac{h^4}{12}\sum_{i=1}^{m}\sum_{j=1}^{m}(f_t'^2(\eta_i,\eta_j) + f_s'^2(\eta_i,\eta_j)) \\ &\leq \frac{h^2}{12}\left(\sup_{(x,y)\in A}|f_t'(x,y)|^2 + \sup_{(x,y)\in A}|f_s'(x,y)|^2\right), \end{aligned} \tag{38}$$

or:

$$\|e(t,s)\| \leq \frac{h}{2\sqrt{3}}\left(\|f_t'\|_\infty^2 + \|f_s'\|_\infty^2\right)^{\frac{1}{2}},$$

hence, $\|e(s,t)\| = O(h)$. □

Theorem 3. Let $X(t)$ and $\hat{X}(t)$ be solutions of Equations (25) and (26), respectively, and let $\|X(t)\| < C$ and $\|k_i\| < C$ for $i = 1,2,3$. Then:

$$E(\left\|X(t) - \hat{X}(t)\right\|^2) \leq O(h^2),$$

where $t \in [0,T)$, $\tau \in [0,1)$; and:

$$\sup_{0\leq\tau<Z}(E(\left\|X(t) - \hat{X}(t)\right\|^2))^{\frac{1}{2}} = O(h^4),$$

where $t \in [0,T)$, $\tau \in [0,1]$.

Proof. We then conduct an error analysis in two ways:

(1.) On the basis of Equation (25), which we express as:

$$\begin{aligned} X(t)-\hat{X}(t) = f(t)-\hat{f}(t) &+ \left(\int_0^t k_1(t,s)X(s-\tau) - \int_0^t \hat{k_1}(t,s)\hat{X}(s-\tau)\right)ds \\ &+ \left(\int_0^t k_2(t,s)X(s-\tau) - \int_0^t \hat{k_2}(t,s)\hat{X}(s-\tau)\right)ds \\ &+ \left(\int_0^t k_2(t,s) - \int_0^t \hat{k_3}(t,s)\right)dB(s), \end{aligned}$$

and taking into account the Euclidean norm:

$$\begin{aligned} E\left\|X(t)-\hat{X}(t)\right\|^2 = E\Bigg\| f(t)-\hat{f}(t) &+ \left(\int_0^t k_1(t,s)X(s-\tau) - \int_0^t \hat{k_1}(t,s)\hat{X}(s-\tau)\right)ds \\ &+ \left(\int_0^t k_2(t,s)X(s-\tau) - \int_0^t \hat{k_2}(t,s)\hat{X}(s-\tau)\right)ds \\ &+ \left(\int_0^t k_3(t,s) - \int_0^t \hat{k_3}(t,s)\right)dB(s)\Bigg\|^2, \end{aligned}$$

and $(a+b+c+d)^2 \leq 4(a^2+b^2+c^2+d^2)$, we obtain:

$$\begin{aligned} \leq 4\Bigg(E\left\|f(t)-\hat{f}(t)\right\|^2 &+ E\left\|\int_0^t k_1(t,s)X(s-\tau) - \int_0^t \hat{k_1}(t,s)\hat{X}(s-\tau)\right\|^2 ds \\ &+ E\left\|\int_0^t k_2(t,s)X(s-\tau) - \int_0^t \hat{k_2}(t,s)\hat{X}(s-\tau)\right\|^2 ds \\ &+ E\left\|\int_0^t k_3(t,s) - \int_0^t \hat{k_3}(t,s)\right\|^2 dB(s)\Bigg). \end{aligned}$$

The final parts are then obtained, one by one:

$$\begin{aligned} I_1 &= \|k_1\| + \|k_2\| \\ &= E\left\|\int_0^t k_1(t,s)X(s-\tau) - \int_0^t \hat{k_1}(t,s)\hat{X}(s-\tau)\right\|^2 ds \\ &= E\left\|\left(\int_0^t k_1(t,s)X(s-\tau) - \int_0^t \hat{k_1}(t,s)X(s-\tau)\right) + \left(\int_0^t \hat{k_1}(t,s)X(s-\tau) - \int_0^t \hat{k_1}(t,s)\hat{X}(s-\tau)\right)\right\|^2 \\ &\leq 2E\left\|\int_0^t [k_1(t,s)-\hat{k_1}(t,s)]X(s-\tau)ds\right\|^2 + 2E\left\|\hat{k_1}(t,s)[X(s-\tau)-\hat{X}(s-\tau)ds]\right\|^2. \\ &\leq C\int_0^t E||k_1(t,s)-\hat{k_1}(t,s)||^2 ds + C\int_0^t \left(E||X(s-\tau)-\hat{X}(s-\tau)||\right)ds \\ &\leq C\cdot O(h^4) + C\cdot O(h^4) = O(h^4). \end{aligned}$$

$\|k_2\|$ is omitted since the steps are similar to $\|k_1\|$.

And:

$$I_2 = E\left\|\int_0^t k_3(t,s) - \hat{k_3}(t,s)\right\|^2 dBs = \int_0^t E(\left\|k_3(t,s)-\hat{k_3}(t,s)\right\|)ds \leq O(h^4),$$

(Itô isometry).

Therefore:

$$\begin{aligned} E\left\|X(t)-\hat{X}(t)\right\|^2 ds &\leq 4(O(h^4)+O(h^4)+O(h^4)+O(h^4)), \\ E\left\|X(t)-\hat{X}(t)\right\| &\leq C.O(h^2). \end{aligned}$$

(2.) We express Equation (25) as the basis for the analysis:

$$X(t)-\hat{X}(t)=(f(t)-\hat{f}(t))+\left(\int_0^t k_1(t,s)X(s-\tau)-\int_0^t \hat{k_1}(t,s)\hat{X}(s-\tau)ds\right)+\left(\int_0^t k_2(t,s)X(s-\tau)-\int_0^t \hat{k_2}(t,s)\hat{X}(s-\tau)ds\right)+\left(\int_0^t k_3(t,s)X(s-\tau)-\int_0^t \hat{k_3}(t,s)\hat{X}(s-\tau)\right)dB(s),$$

in addition to getting the Euclidean norm:

$$\left\|X(t)-\hat{X}(t)\right\|^2=||f(t)-\hat{f}(t)||^2+\left\|\int_0^t k_1(t,s)X(s-\tau)-\int_0^t \hat{k_1}(t,s)\hat{X}(s-\tau)ds\right\|^2+\left\|\int_0^t k_2(t,s)X(s-\tau)-\int_0^t \hat{k_2}(t,s)\hat{X}(s-\tau)ds\right\|^2+\left\|\int_0^t k_3(t,s)X(s-\tau)-\int_0^t \hat{k_3}(t,s)\hat{X}(s-\tau)\right\|^2 dB(s),$$

and:

$$E(\left\|X(t)-\hat{X}(t)\right\|^2)\leq 4\Bigg(\ E||f(t)-\hat{f}(t)||^2+E\left\|\int_0^t k_1(t,s)X(s-\tau)-\int_0^t \hat{k_1}(t,s)\hat{X}(s-\tau)ds\right\|^2+E\left\|\int_0^t k_2(t,s)X(s-\tau)-\int_0^t \hat{k_2}(t,s)\hat{X}(s-\tau)ds\right\|^2+E\left\|\int_0^t k_3(t,s)X(s-\tau)-\int_0^t \hat{k_3}(t,s)\hat{X}(s-\tau)\right\|^2 dB(s)\ \Bigg).$$

The Itô isometry property [22] and Rolle's theorem lead to the following results:

$$\begin{aligned}
&\leq CE\left(\left\|f(t)-\hat{f}(t)\right\|^2\right)\\
&-4\int_0^t E\left(\left\|(k_1(t,s)-\hat{k_1}(t,s))(X(s-\tau))\right\|^2\right)ds-4\int_0^t E\left(\left\|\hat{k_1}(t,s)(X(s-\tau)-\hat{X}(s-\tau))\right\|^2\right)\\
&+6\int_0^t E\left(\left\|(k_2(t,s)-\hat{k_2}(t,s))(X(s-\tau))\right\|^2\right)ds+6\int_0^t E\left(\left\|\hat{k_2}(t,s)(X(s-\tau)-\hat{X}(s-\tau))\right\|^2\right)\\
&-4\int_0^t E\left(\left\|(k_3(t,s)-\hat{k_3}(t,s))\hat{X}(s-\tau)\right\|^2\right)ds-4\int_0^t E\left(\left\|\hat{k_3}(t,s)(X(s-\tau)-\hat{X}(s-\tau))\right\|^2\right)ds.
\end{aligned}$$

Based on the problem:

$$\begin{aligned}
&\leq CE(\left\|f(t)-\hat{f}(t)\right\|^2)\\
&-4C^3\int_0^t E\left(\left\|(k_1(t,s)-\hat{k_1}(t,s))\right\|^2\right)ds-4C^3\int_0^t E\left(\left\|X(s)-\hat{X}(s)\right\|^2\right)ds\\
&+6C^2\int_0^t E\left(\left\|(k_2(t,s)-\hat{k_2}(t,s))\right\|^2\right)ds+6C^2\int_0^t E\left(\left\|X(s)-\hat{X}(s)\right\|^2\right)ds\\
&-4C^3\int_0^t E\left(\left\|(k_3(t,s)-\hat{k_3}(t,s))\right\|^2\right)ds-4C^3\int_0^t E\left(\left\|(X(s-\tau)-\hat{X}(s-\tau))\right\|^2\right)ds,
\end{aligned}$$

and the proof is complete. Hence:

$$E\left(\left\|X(t)-\hat{X}(t)\right\|^2\right)\leq O(h^2). \qquad \square$$

6. Numerical examples

To illustrate the method stated in Section 5, we consider the following examples. The computations associated with the examples were performed using Python 3. Let X_i denote the block pulse coefficient of the exact solution in the given examples, and let Y_i be the block pulse coefficient of computed solutions by the presented method.

We compute the values of approximate and exact solutions at selected points defined as $\tau=(q+\lambda)h$ and $\|E\|_\infty=\max_{1\leq i\leq m}|X_i-Y_i|$.

n	$\bar{\chi}_E$	S_E	95 % confidence interval for mean of E	
			Lower	Upper
50	0.00382054	0.00283136	0.00330007	0.00434101
100	0.00370446	0.00263633	0.00337978	0.00402914
150	0.00371797	0.00263859	0.00345360	0.00398234
200	0.00376432	0.00271663	0.00352496	0.00400368
250	0.00377341	0.00266278	0.00356629	0.00398054
300	0.00376643	0.00253417	0.00348075	0.00495210

TABLE 1. Mean, standard deviation, and mean confidence interval for error in example 1 with $m = 32$, $q = 0$, $\lambda = 0.1$.

n	$\bar{\chi}_E$	S_E	95 % confidence interval for mean of E	
			Lower	Upper
50	0.19111046	0.10332342	0.16174627	0.22047465
100	0.19936926	0.09891785	0.17974181	0.21899671
150	0.19952633	0.09352666	0.18443667	0.21461600
200	0.19786280	0.09228118	0.18499526	0.21073033
250	0.19378207	0.08840576	0.18276985	0.20479428
300	0.19387334	0.08744348	0.18393814	0.20380853

TABLE 2. Mean, standard deviation, and mean confidence interval for error in example 1 with $m = 64$, $q = 0$, $\lambda = 0.1$.

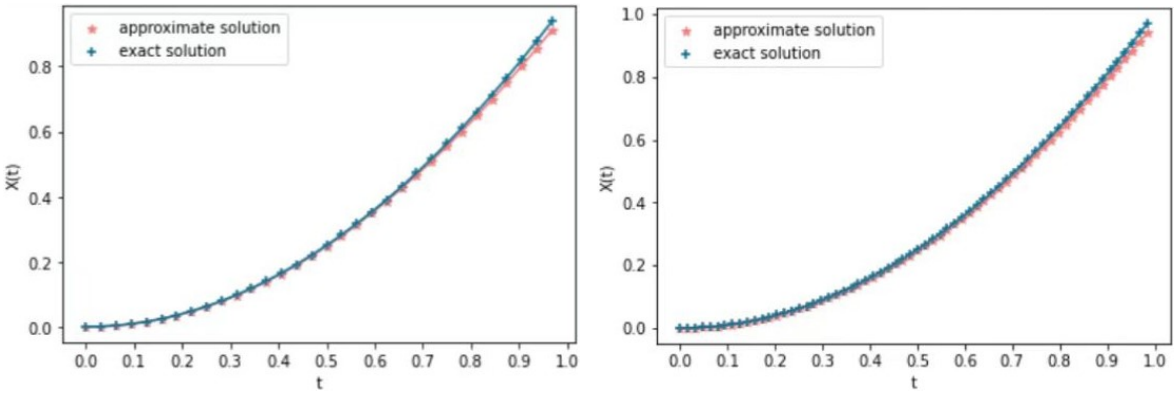

FIGURE 1. The trajectory of the approximate solution and exact solution of Example 1 for $m = 32$, $m = 64$, $n = 50$, $q = 0$, $\lambda = 0.5$.

Example 1 [16]. Consider the following stochastic Volterra Integral equation with (constant) time delay $\tau > 0$:

$$X(t) = -\frac{t^4}{12} + \frac{t^3}{3}\tau + (1 - \frac{\tau^2}{2})t^2 + \int_0^t (t-s)X(s-\tau)ds, \tag{39}$$

where $s, t \in [0, T]$, $\tau \in (0, T)$; with the exact solution $X(t) = t^2$, for $0 \leq t \leq T$.

In Tables 1–2, the numerical results are presented. The computations of mean, standard deviation, and mean confidence interval of error for n, $\bar{\chi}_E$, and S_E are provided in Tables 1–2. An approximate solution is depicted in Figure 1 as a trajectory based on the presented approach. The variation process of error is represented by curves in Figure 2. We observe a perfect agreement between the exact solution and the numerical results, achieving full convergence.

Example 2 [16]. Consider the following Fredholm integral equation with (constant) time delay $\tau > 0$:

$$X(t) = t(T\cos(T-\tau) - \sin(T-\tau) - \sin(\tau)) + \sin(t) + \int_0^T (ts)X(s-\tau)ds, \tag{40}$$

where $s, t \in [0, T]$, $\tau \in (0, T)$; with the exact solution $X(t) = \sin(t)$, for $0 \leq t \leq T$. The numerical results are presented in Table 3. The trajectory of the approximate solution and exact solution are represented in Figures 3–7.

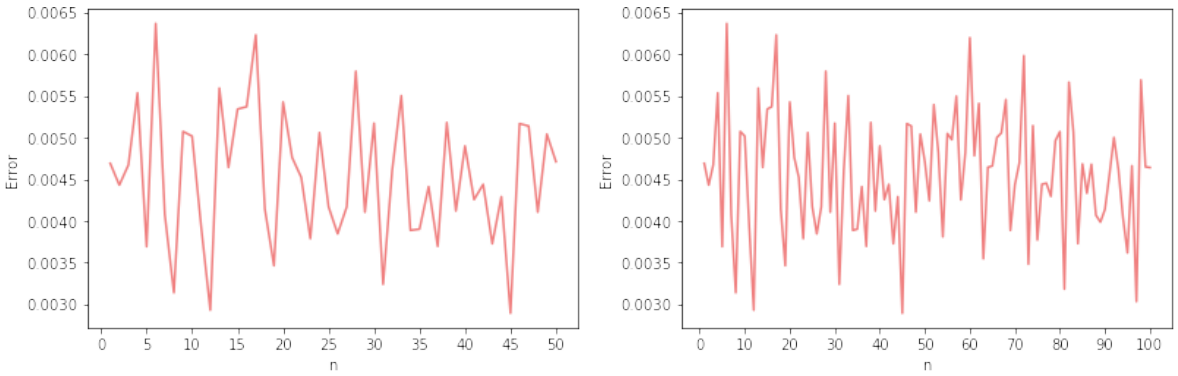

Figure 2. Variation trend of error in Example 1 for $m = 32$, $n = 50$, $n = 100$, $q = 0$, $\lambda = 0.5$.

	$\lambda = 0.1$	$\lambda = 0.3$	$\lambda = 0.5$	$\lambda = 0.7$	$\lambda = 0.9$
$m = 8$	0.007788	0.007251	0.006711	0.00727	0.008367
$m = 32$	0.015303	0.015683	0.016064	0.016446	0.016827
$m = 64$	0.017717	0.017918	0.01812	0.018321	0.018523

Table 3. Error in Example 2 with $q = 0$.

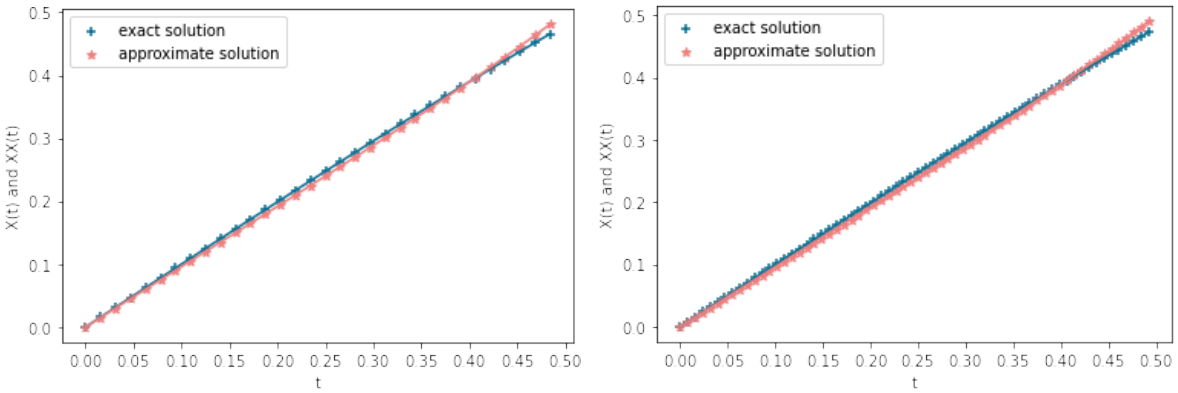

Figure 3. The trajectory of the approximate solution and exact solution of Example 2 for $m = 32$, $m = 64$, $n = 50$, $q = 0$, $\lambda = 0.1$.

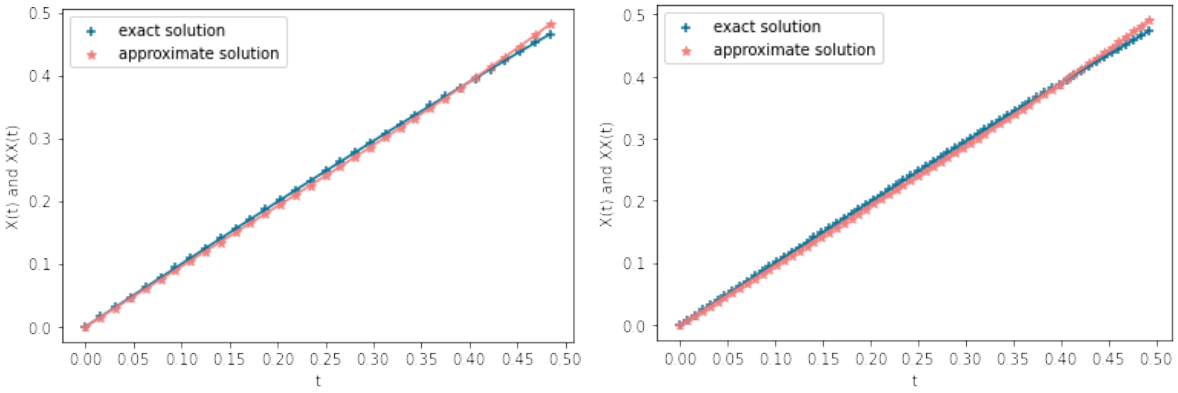

Figure 4. The trajectory of the approximate solution and exact solution of Example 2 for $m = 32$, $m = 64$, $n = 50$, $q = 0$, $\lambda = 0.3$.

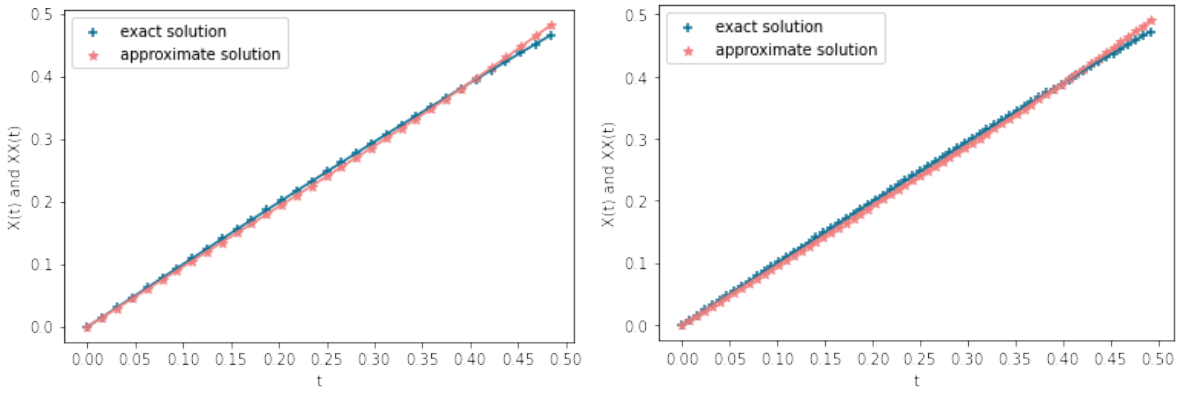

FIGURE 5. The trajectory of the approximate solution and exact solution of Example 2 for $m = 32$, $m = 64$, $n = 50$, $q = 0$, $\lambda = 0.5$.

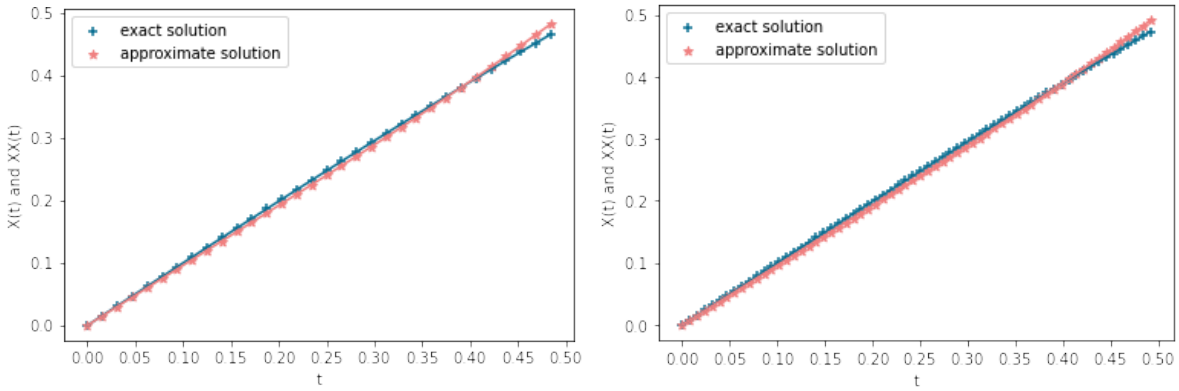

FIGURE 6. The trajectory of the approximate solution and exact solution of Example 2 for $m = 32$, $m = 64$, $n = 50$, $q = 0$, $\lambda = 0.7$.

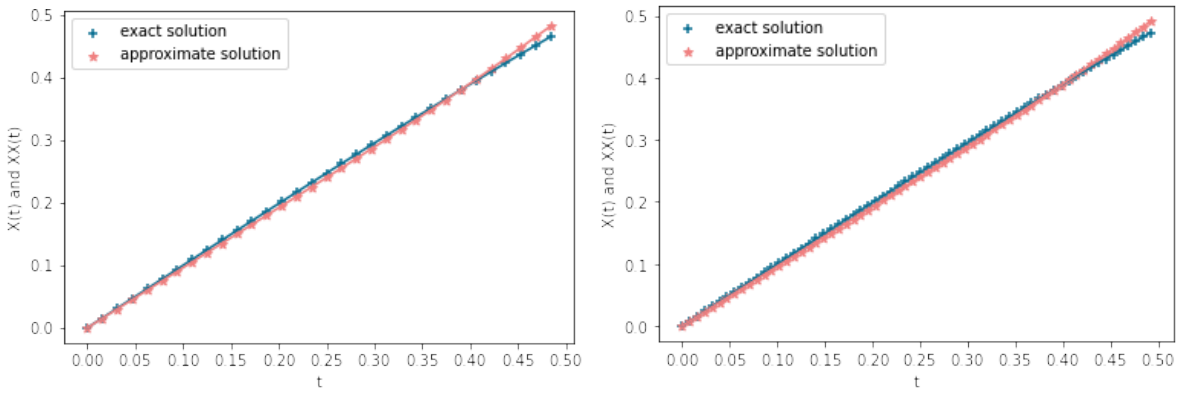

FIGURE 7. The trajectory of the approximate solution and exact solution of Example 2 for $m = 32$, $m = 64$, $n = 50$, $q = 0$, $\lambda = 0.9$.

Example 3 [28]. Consider the stochastic Volterra Fredholm integral equation with time delay $\tau > 0$:

$$X(t) = -5\tau - t + 12t^2 - t^3 - t^4\tau + \int_0^t (t-s)X(s-\tau)ds + \int_0^1 (t+s)X(s-\tau)ds + \int_0^t sX(s-\tau)dB(s), \quad (41)$$

where $s, t \in [0, T]$, $\tau \in (0, T)$; with the exact solution $X(t) = \exp\left((6t + 12t^2)/2 + \int_0^t sdB(s)\right)$, $\{B(t) : 0 \leq t \leq T\}$ is a Brownian motion process, and $X(t)$ is an unknown stochastic process defined on the probability space $(\Omega, \mathbb{F}, \mathbb{P})$. Tables 4–5 present numerical results for various values of m, for $\lambda = 0.5$ to compute the τ.

7. Conclusion

It is possible to use a computational method based on the properties of BPFs with operational matrices to convert the problem into a system of linear algebraic equations. As a result, this technique transforms nonlinear

n	$\bar{\chi}_E$	S_E	95 % confidence interval for mean of E	
			Lower	Upper
50	0.19136844	0.06088437	0.17406529	0.20867159
100	0.18904432	0.06630608	0.17588776	0.20220088
150	0.18060058	0.06734891	0.16973445	0.19146671
200	0.18457774	0.07436710	0.17420811	0.19494736
250	0.18513391	0.07368228	0.17595571	0.19431210
300	0.18425841	0.07426964	0.17582001	0.19269681

Table 4. Mean, standard deviation, and mean confidence interval for error in Example 3 with $m = 32$, $q = 0$, $\lambda = 0.5$.

n	$\bar{\chi}_E$	S_E	95 % confidence interval for mean of E	
			Lower	Upper
50	0.18850030	0.07900637	0.16604694	0.21095366
100	0.19126831	0.07912381	0.17556843	0.20696819
150	0.19011608	0.08055573	0.17711915	0.20311301
200	0.19260138	0.08272020	0.18106700	0.20413575
250	0.18888323	0.08117339	0.17877191	0.19899455
300	0.18898994	0.08172767	0.17970417	0.19827572

Table 5. Mean, standard deviation, and mean confidence interval for error in Example 3 with $m = 64$, $q = 0$, $\lambda = 0.5$.

stochastic Volterra-Fredholm integral equations into a system of linear algebraic equations whose coefficients represent BPFs that represent solutions to these equations. As well as error analysis, numerical examples provide a solid basis for combined effects and observe a perfect agreement between the exact solutions and the numerical results, achieving full convergence. These include stochastic integrals and ordinary differential equations; arithmetic operations are carried out without requiring derivatives or integration. A Python 3 environment was used to perform the computations associated with the examples. We observe the auspicious results and hope to extend the method to more general backward stochastic Volterra integral equations in sequels.

Acknowledgements

The authors thank the reviewers for their valuable comments and efforts to improve our article. This research was supported by National Key R&D Program of China (2023YFA1008903) and the Major Fundamental Research Project of Shandong Province of China (No. ZR2023DZ33).

References

[1] H. K. Dawood. Computational block-pulse functions method for solving Volterra integral equations with delay. *Journal of University of Babylon for Pure and Applied Sciences* **27**(1):32–42, 2019. https://doi.org/10.29196/jubpas.v27i1.2063

[2] C. Kasumo. On the approximate solutions of linear Volterra integral equations of the first kind. *Applied Mathematical Sciences* **14**(3):141–153, 2020. https://doi.org/10.12988/ams.2020.912176

[3] K. Maleknejad, P. Torabi, S. Sauter. Numerical solution of a non-linear Volterra integral equation. *Vietnam Journal of Mathematics* **44**:5–28, 2016. https://doi.org/10.1007/s10013-015-0149-8

[4] E. Babolian, Z. Masouri. Direct method to solve Volterra integral equation of the first kind using operational matrix with block-pulse functions. *Journal of Computational and Applied Mathematics* **220**(1–2):51–57, 2008. https://doi.org/10.1016/j.cam.2007.07.029

[5] T. S. Gutleb, S. Olver. A sparse spectral method for Volterra integral equations using orthogonal polynomials on the triangle. *SIAM Journal on Numerical Analysis* **58**(3):1993–2018, 2020. https://doi.org/10.1137/19M1267441

[6] Y. Hamaguchi. On the maximum principle for optimal control problems of stochastic Volterra integral equations with delay. *Applied Mathematics & Optimization* **87**:42, 2023. https://doi.org/10.1007/s00245-022-09958-w

[7] K. Maleknejad, K. Mahdiani. Solving nonlinear mixed Volterra-Fredholm integral equations with two dimensional block-pulse functions using direct method. *Communications in Nonlinear Science and Numerical Simulation* **16**(9):3512–3519, 2011. https://doi.org/10.1016/j.cnsns.2010.12.036

[8] M. Rabbani, K. Nouri. Solution of integral equations by using block-pulse functions. *Mathematical Sciences Quarterly Journal* **4**(1):39–48, 2010.

[9] S. H. Esmail Babolian, Zahra Masouri. New direct method to solve nonlinear Volterra-Fredholm integral and integro-differential equations using operational matrix with block-pulse functions. *Progress In Electromagnetics Research B* **8**:59–76, 2008. https://doi.org/10.2528/PIERB08050505

[10] Y. Shi, T. Wang. Solvability of general backward stochastic Volterra integral equations. *Journal of the Korean Mathematical Society* **49**(6):1301–1321, 2012. https://doi.org/10.4134/JKMS.2012.49.6.1301

[11] A. A. Khidir. A numerical technique for solving Volterra-Fredholm integral equations using Chebyshev spectral method. *Ricerche di Matematica* 2022. https://doi.org/10.1007/s11587-022-00692-7

[12] M. Samar, K. E. Yao, X. Zhu. Numerical solution of nonlinear backward stochastic Volterra integral equations. *Axioms* **12**(9):888, 2023. https://doi.org/10.3390/axioms12090888

[13] A. Bellour, M. Bousselsal. A Taylor collocation method for solving delay integral equations. *Numerical Algorithms* **65**(4):843–857, 2014. https://doi.org/10.1007/s11075-013-9717-8

[14] Q. Zhu, T. Huang. Stability analysis for a class of stochastic delay nonlinear systems driven by G-Brownian motion. *Systems & Control Letters* **140**:104699, 2020. https://doi.org/10.1016/j.sysconle.2020.104699

[15] R. Song, B. Wang, Q. Zhu. Stabilization by variable-delay feedback control for highly nonlinear hybrid stochastic differential delay equations. *Systems & Control Letters* **157**:105041, 2021. https://doi.org/10.1016/j.sysconle.2021.105041

[16] M. Nouri, K. Maleknejad. Numerical solution of delay integral equations by using block pulse functions arises in biological sciences. *International Journal of Mathematical Modelling & Computations* **6**(3):221–232, 2016.

[17] F. Toutounian, E. Tohidi, A. Kilicman. Fourier operational matrices of differentiation and transmission: Introduction and applications. *Abstract and Applied Analysis* **2013**:198926, 2013. https://doi.org/10.1155/2013/198926

[18] J. Zhang, Y. Li, J. Xie. Numerical simulation of fractional control system using Chebyshev polynomials. *Mathematical Problems in Engineering* **2018**:4270764, 2018. https://doi.org/10.1155/2018/4270764

[19] F. Stenger. *Numerical Methods Based on Sinc and Analytic Functions*, vol. 20. Springer New York, 1993. ISBN 978-1-4612-7637-1. https://doi.org/10.1007/978-1-4612-2706-9

[20] Z. Jiang, W. Schaufelberger. *Block Pulse Functions and Their Applications in Control Systems*. Springer-Verlag, Berlin, 1992. ISBN 978-3-540-55369-4. https://doi.org/10.1007/BFb0009162

[21] G. P. Rao. *Piecewise Constant Orthogonal Functions and Their Application to Systems and Control*. Springer-Verlag, Berlin, 1983. ISBN 978-3-540-12556-3. https://doi.org/10.1007/BFb0041228

[22] F. C. Klebaner. *Introduction to Stochastic Calculus with Applications*. Imperial College Press, 3rd edn., 2012. ISBN 978-1-84816-831-2. https://doi.org/10.1142/p821

[23] M. Khodabin, K. Maleknejad, M. Rostami, M. Nouri. Numerical approach for solving stochastic Volterra-Fredholm integral equations by stochastic operational matrix. *Computers & Mathematics with Applications* **64**(6):1903–1913, 2012. https://doi.org/10.1016/j.camwa.2012.03.042

[24] M. A. Hussein, H. K. Jassim. Analysis of fractional differential equations with Antagana-Baleanu fractional operator. *Progress in Fractional Differentiation and Applications* **9**(4):681–686, 2023. https://doi.org/10.18576/pfda/090411

[25] H. K. Jassim, M. A. Hussein, M. R. Ali. An efficient homotopy permutation technique for solving fractional differential equations using Atangana-Baleanu-Caputo operator. *AIP Conference Proceedings* **2845**(1):060008, 2023. https://doi.org/10.1063/5.0157148

[26] V. Horvat. On collocation methods for Volterra integral equations with delay arguments. *Mathematical Communications* **4**(1):93–109, 1999.

[27] M. Mosleh, M. Otadi. Least squares approximation method for the solution of Hammerstein-Volterra delay integral equations. *Applied Mathematics and Computation* **258**:105–110, 2015. https://doi.org/10.1016/j.amc.2015.01.100

[28] J.-H. He, M. H. Taha, M. A. Ramadan, G. M. Moatimid. Improved block-pulse functions for numerical solution of mixed Volterra-Fredholm integral equations. *Axioms* **10**(3):200, 2021. https://doi.org/10.3390/axioms10030200